Tracking rates of ecotone migration due to salt-water encroachment using fossil mollusks in coastal South Florida.

Evelyn E. Gaiser[1,2,*], Angelikie Zafiris[1], Pablo L. Ruiz[2], Franco A. C. Tobias[2], and Michael S. Ross[2]

[1]*Department of Biological Sciences, Florida International University, Miami, FL 33199*

[2]*Southeast Environmental Research Center, Florida International University, Miami, FL 33199*

([*]Author for correspondence: E-mail: gaisere@fiu.edu)

Key words: Mangroves, sea-level rise, salt-water encroachment, paleoecology, mollusks, Everglades, coastal wetlands

Note: This paper has not been submitted elsewhere in identical or similar form, nor will it be during the first three months after its submission to *Hydrobiologia*.

Abstract

We determined the rate of migration of coastal vegetation zones in response to salt-water encroachment through paleoecological analysis of mollusks in 36 sediment cores taken along transects perpendicular to the coast in a 5.5 km^2 band of coastal wetlands in southeast Florida. Five vegetation zones, separated by distinct ecotones, included freshwater swamp forest, freshwater marsh, and dwarf, transitional and fringing mangrove forest. Vegetation composition, soil depth and organic matter content, porewater salinity and the contemporary mollusk community were determined at 226 sites to establish the salinity preferences of the mollusk fauna. Calibration models allowed accurate inference of salinity and vegetation type from fossil mollusk assemblages in chronologically calibrated sediments. Most sediments were shallow (20-130 cm) permitting coarse-scale temporal inferences for three zones: an upper peat layer (zone 1) representing the last 30-70 years, a mixed peat-marl layer (zone 2) representing the previous ca. 150-250 years and a basal section (zone 3) of ranging from 310 to 2990 YBP. Modern peat accretion rates averaged 3.1 mm yr^{-1} while subsurface marl accreted more slowly at 0.8 mm yr^{-1}. Salinity and vegetation type for zone 1 show a steep gradient with freshwater communities being confined west of a north-south drainage canal constructed in 1960. Inferences for zone 2 (pre-drainage) suggest that freshwater marshes and associated forest units covered 90 % of the area, with mangrove forests only present along the peripheral coastline. During the entire pre-drainage history, salinity in the entire area was maintained below a mean of 2 ppt and only small pockets of mangroves were present; currently, salinity averages 13.2 ppt and mangroves occupy 95% of the wetland. Over 3 km^2 of freshwater wetland vegetation type have been lost from this basin due to salt-water encroachment, estimated from the mollusk-inferred migration rate of freshwater

vegetation of 3.1 m yr^{-1} for the last 70 years (compared to 0.14 m yr^{-1} for the pre-drainage period). This rapid rate of encroachment is driven by sea-level rise and freshwater diversion. Plans for rehydrating these basins with freshwater will require high-magnitude re-diversion to counteract locally high rates of sea-level rise.

Introduction

Coastal wetland ecosystems are being reduced at alarming rates due to losses on their marine margins resulting from sea-level rise and on their interior margins as a result of urban or agricultural expansion (IPCC, 1998). Sea level has risen 10 to 25 centimeters in the past 100 years, and it is predicted to rise another 50 centimeters over the next century (Church et al., 2001), linked with the increase in global atmospheric temperature. An estimate by Nicholls et al. (1999) suggests that accelerating rates of sea-level rise could cause the loss of as much as 22% of the world's coastal wetlands by the end of the 21st century. Manipulation of the landscape, particularly of the path of water flow through coastal estuaries, by industrialization and urban expansion in the coastal zone has further reduced the extent of natural coastal wetland vegetation (National Research Council, 1993; Park et al., 1989).

Of the many examples of coastal wetland losses due to these two factors, one of the most striking is the decline in wetlands along Florida's Atlantic coast, where the rate of sea-level rise is more than double the global average (2-4 mm yr^{-1}, Leatherman et al., 2000) and routes of water flow through adjoining Everglades wetlands have been engineered for drainage purposes, thereby facilitating high rates of urban expansion. The effects of the latter on coastal wetlands exceed the former, as freshwater draining to the coast has been channelized into a vast network of canals, constructed during the last century to expand agriculture and urban development. Along the southeast Florida coastline, this process has resulted in the loss of most of the myriad of natural east-west draining creeks that meandered from the Everglades to the coast, hydrating coastal wetlands with freshwater (Meeder et al., 2000). Now, water is channelized into point-

source discharges at the mouths of canals, causing a redistribution of salinity at the coastal wetland-marine interface, i.e., low near canal outlets (especially in the wet season when flood-control structures are open) and much higher in interior coastal wetlands (Boyer et al., 1999; Ross et al., 2000).

Salt-water encroachment threatens the once extensive estuarine wetland system along the edge of the Atlantic coastline. In the 1940's, prior to the construction of the majority of drainage canals in the southern Everglades, Egler (1952) conducted a vegetation survey in these wetlands that he called the "Southeast Saline Everglades." He was able to distinguish distinct vegetation zones lying in bands parallel to the coast, driven by gradients of salinity, water availability, nutrients and susceptibility to drought, periodic freeze events and fire. He identified a coastward sequence of graminoid freshwater wetlands furthest inland, followed by dwarf mangrove scrub swamps in the supratidal positions, and fringing mangrove forest in the intertidal zone adjacent to the coast. Ross et al. (2000) repeated Egler's vegetation survey a half-century later and supplemented interpretations of the magnitude of vegetation change by comparing modern aerial photographs of the area to archived photos available from 1938 and 1940. During the period between these two studies, an extensive network of drainage canals had been constructed to connect the larger South Dade Conveyance system to the sea through the southeast saline Everglades. Completed in the late 1960's, this project allowed more effective drainage of the agricultural and urban lands abutting the coastline. In conjunction with roads and agricultural ditches, operation of the canal system altered fresh water delivery to the wetlands, starving some areas of water while augmenting the supply to others. By the turn of the 21st century, freshwater gramminoid

marshes had been largely displaced by an enroaching mangrove scrub community and most tidal creeks had disappeared (Ross et al., 2000).

In a related study, Ross et al. (2001) determined the distribution patterns of vegetation, epifauna and periphyton (existing here as benthic mats of primarily cyanobacteria, bacteria and diatoms) along a 4 km transect that ran perpendicular to the coast. The interior-most point along the transect was stationed adjacent to a north-south canal that runs parallel to the coastline and prevents coastward movement of freshwater. Marshes to the west of the canal were dominated by communities typical of the freshwater Everglades, including sawgrass (*Cladium jamaicense* Crantz) and spikerush (*Eleocharis cellulosa* Torr.). Immediately east of the canal these communities were replaced by a salt-tolerant gramminoid community dominated by *Juncus romoerianus* Scheele and *Distichilis spicata* (L.), which was replaced coastward by a broad zone of very unproductive, sparse dwarf red mangrove (*Rhizophora mangle* L.) and thick benthic periphyton mats. Finally, the coastline was fringed with highly productive, tall-statured mangroves (including *R. mangle*, *Avicennia germinans* (L.), *Laguncularia racemosa* Gatern. and *Conocarpus erecta* L.). The zone of low productivity sandwiched between the graminoid marsh and fringing mangroves reflects white on aerial photographs and, through comparison with 1940 aerial photographs, this "white zone" was determined to have moved interior-ward by 1.5 km, effectively shrinking the graminoid communities that had formerly been present east of the canal (Ross et al., 2000).

Ross et al. (2001) also found the distribution of diatoms in periphyton mats and mollusks to be highly correlated with distance from the coastline. A unique community of each existed in the

freshwater graminoid marsh, the salt-tolerant graminoid marsh, the white zone and the fringing mangrove forest. Salinity preferences were determined for 154 diatom and 17 mollusk taxa for future monitoring efforts and paleoecological studies (Gaiser et al., 2004). However, diatoms were found to be poorly preserved in subsurface coastal sediments while mollusks were well preserved and abundant in sediments (Ross et al., 2001).

Such evidence of rapid of salt-water encroachment, with concomitant effects on coastal wetland community composition, have provided a foundation of support for allocation of state and federal funding toward restoration of coastal wetlands, as part of the Comprehensive Everglades Ecosystem Restoration Program (the largest restoration program ever undertaken by the U.S. Federal Government). Restoration largely depends on the magnitude of freshwater that can be re-diverted back into the coastal wetlands, although re-diversion may have diminishing impact as it is counteracted by the opposing effects of sea-level rise. It is, therefore, imperative to understand the magnitude of influence of freshwater diversion on salt-water encroachment in the context of that caused by sea-level rise. Our approach in this study was to determine rates at which ecotones have shifted along the South Florida coastline since channelization efforts began in the early 1900's, in contrast to pre-development rates during the ~2000 year history of this wetland basin. We used a paleoecological approach, focusing on mollusks as our major paleoenvironmental proxy, as they can be excellent indicators of environmental change in coastal ecosystems (Ross et al., 2001; Brewster-Wingard et al., 2001). Specifically, our goals were to (1) determine the current composition of mollusk communities in the BBCW and their relationship to coastal zones defined by vegetation community composition, salinity and soil character, and

(2) interpret the location of these zones using fossil mollusk communities to determine rates of ecotonal migration due to the combined forces of sea-level rise and freshwater diversion.

Materials and methods

Study site description

The present study focuses on an area of remnant coastal wetlands within the Biscayne Bay Coastal Wetlands in the southeast saline Everglades (Fig. 1). The ~7 km long study area, part of which is protected in Biscayne National Park, is bounded on the north and south by major east-west drainage canals (Princeton and Mowry Canals, respectively) and bisected north-south by a secondary canal (L-31E). The region is dissected by many smaller east-west ditches which compartmentalize it longitudinally into 13 hydrologically distinct wetland basins, ranging in width from about 0.5 to 2 km. To the west of the L-31E canal, freshwater marshes are now hydrologically isolated from the coast and bounded to the west by agricultural lands, the periphery of which are heavily invaded by exotic trees including *Schinus terebinthifolius* Raddi (Brazilian Peppertree) and *Casuarina equisetifolia* L. (Australian Pine). East of the L-31E canal, mangrove communities predominate, with strands of forest vegetation now occupying the remnant tidal creek beds. Though each sub-basin contains a gradation of freshwater to marine communities from the interior to the coast, the distinctiveness of the zones, the abruptness and location of the ecotonal boundaries and their specific composition vary somewhat among sub-basins.

Distribution of modern communities

To determine the current distribution of mollusks relative to existing patterns of vegetation, soils and salinity in the BBCW, we used a stratified-random design to select study sites within the 13 sub-basins (numbered consecutively from south to north, Fig. 1). Using aerial photos of the area, each sub-basin was divided into 4-6 units. To the west of the L-31E canal, a freshwater swamp forest was dominated by exotics that have invaded abandoned agricultural land and remnant freshwater graminoid marsh. East of the canal, vegetation was primarily mangrove forests that can be characterized by canopy height and cover as dwarf, transitional and fringing (along the coastline). Occasionally a sub-basin did not include one or more of these components or another community type was present, in which case the sub-basin was divided accordingly such that each unit was equally represented in sampling. Within each unit a north-south transect was randomly located, and 1-5 sampling stations were evenly distributed along its length. A total of 226 stations were sampled within the 5.5 km^2 area (Fig. 1a), with each site being visited once in the dry season during February- June 2002 and 2003.

A nested design was used to describe vegetation using the following procedure. A 10-meter N-S transect was established at each point. For trees (stems >2 meters height), we recorded the species and diameter class (5-cm DBH ranges) of all live and dead individuals within one meter of the line (stems <10 cm DBH), two meters of the line (stems 10-25 cm DBH), and five meters of the line (>25 cm DBH). We recorded the species and diameter class of all dead fallen stems (> 5 cm DBH) whose trunk intersected the line. We estimated live cover by species in a 4-meter-wide band enclosing the center line, using the following cover classes: 1, 0-1%; 2, 1-4%;

3, 4-16%; 4, 16-33%; 5, 33-66%; and 6, >66%. Finally, we recorded the upper and lower height of each species that intercepted or was within 1 meter of a height pole positioned vertically at three locations along the centerline, i.e., 0, 5, and 10 meters from the origin. For shrubs (woody stems between 60 cm and 2 meters in height), we recorded the density of all stems in five 1-m^2 plots established at five locations along the center line, i.e., west of the line, at 0, 2, 4, 6, and 8 meters from the origin. Stems were counted by species in two size categories: small shrubs (60-100 cm tall) and large shrubs (1-2 m tall). For seedlings (woody stems 0-60 cm in height), we recorded the density of all stems in a 3 x 3 dm subplot in the southeast corner of the 1 m^2 plot described above. Stems were counted by species in two size categories: small seedlings (0-30 cm tall) and large seedlings (30-60 cm tall). For all plants < 2 meters height (herbs, seedlings, shrubs), we estimated cover in the 1 m^2 plots described above, using the same cover classes as described above for trees.

Within each site, we measured depth of sediments to limestone bedrock with a probe-rod and then used a soil auger to extract sediments to measure and describe depths of compositional and textural transitions (i.e., depth of peat was defined for each core). The color transition and composition of the sediments were described using a Munsell color chart. At each site a portable meter was used to measure conductivity in pore water that collected in the hole created after the sediments were extracted. Conductivity ($\mu S\ cm^{-1}$) was later converted to salinity (ppt) using a model from a previous study in a nearby basin where both variables were directly measured (Ross et al., 2001). While porewater salinity is known to vary seasonally, locality differences overwhelm temporal variability such that point measurements can be reliably used as an indication of the site-specific salinity regime (Ross et al., 2001).

From each site, five small sections of benthic periphyton and litter (3.8 cm^2, 1-2 cm thick) were collected using aluminum cores and then combined to form a single sample to determine the distribution of the modern mollusk community. In the laboratory, each sample was gently rinsed with water through a 500 μm sieve and intact mollusks were collected. The mollusks were dried at 80°C for ~3-5 days in order to compare mass quantities and then counted and identified to the species level using standard and local literature (Abbott, 1954; Thompson, 2002). Identifications were later verified by Dr. Rudiger Bieler, Curator of the Field Museum of Natural History, Chicago, IL.

Paleoecological survey

A series of sediment cores were taken along east-west transects in basins 2, 7, 10 and 13 (Fig. 2b). Several additional sites in other basins that showed interesting textural and compositional patterns were also cored, resulting in 36 coring locations (Fig. 2b). Using a soil auger, sediment cores were extracted in sequential sections until bedrock was encountered. In the field, the sediment sections were arranged in sequence according to depth. The transitions in composition and texture of the sediments were described and measured with a meter stick, proceeding from the surface sediments to the bottom. Sub-samples from each distinct layer were removed, placed in plastic bags, and labeled according to depth range. Four to 6 composite samples were removed from each core. In the laboratory, each subsample was washed and mollusks were removed using the same procedure as for the modern samples.

At a subset of 10 of these sites (Fig. 2b), we removed a pair of intact sediment cores using a 7.6 cm diameter, 2-m long aluminum core tube. The base of the core tube was serrated with a saw and then driven into the sediments to bedrock by rotating a cross bar at the top of the tube. The serrated edges were bent inward to seal the base of the sediments by driving the tube into bedrock using a pounding block at the top of the tube. The tube containing sediments was then capped and retrieved using a tripod and winch, positioned above the core. The depth of the bore hole was measured after extraction as well as the length of sediment inside the tube. Cores were returned upright to the laboratory and maintained in a cold room. The core tube was then split lengthwise on both sides using a rotary saw. Sediments were then also sliced lengthwise using pottery wire pulled down the length of the core. Once exposed, sediments were photographed and detailed notes were taken on the stratigraphy of color, texture and content. One of each set of cores was then sliced into 1 cm cross-sections; each section was dried in an 80°C for ~3-5 days to be used for radiometric dating. A subsection was analyzed for organic and carbonate content by first combusting at 500ºC for 1 hr, followed by combustion at 1000ºC for 1 hr.

Radiometric dating

To determine the chronology of these 10 cores, we used a combination of ^{210}Pb and ^{14}C radiometric dating for recent (<ca. 100 YBP) and older (>ca. 100 YBP) sediments. The ^{210}Pb analysis was performed in the laboratory of Dr. Daniel Engstrom, St. Croix Watershed Research Station, MN. Lead-210 was measured on dried material from each 1-cm depth interval through its grand-daughter product ^{210}Po, with ^{209}Po added as an internal yield tracer. The polonium isotopes were distilled from 0.2-1.2 g dry sediment at 550° C following pretreatment with

concentrated HCl and plated directly onto silver planchets from a 0.5 N HCl solution (modified from Eakins & Morrison, 1976). Activity was measured for 1-14 days with ion-implanted detectors and an EG&G Nuclear alpha spectroscopy system. Unsupported ^{210}Pb was calculated by subtracting supported activity from the total activity measured at each level, with supported ^{210}Pb estimated from the asymptotic activity at depth (the mean of the lowermost three samples in the core). Dates and sedimentation rates are determined according to the c.r.s. (constant rate of supply) model (Appleby & Oldfield, 1978) with confidence intervals calculated by first-order error analysis of counting uncertainty (Binford, 1990).

Organic material from the base of 5 of these cores was selected for ^{14}C analysis by Beta Analytic, Miami, FL. Material was examined under a dissecting microscope, and, if large (>1 mm) plant fragments were found, carbon in these fragments was reduced to graphite and ^{14}C measured by accelerated-mass-spectrometry (AMS). Otherwise, carbon in bulk organic material was synthesized to benzene and ^{14}C measured for an extended period of time on a scintillation spectrometer. Conventional ^{14}C age was calculated after applying ^{13}C/^{12}C corrections and ages reported in units YBP, where 'present' is defined as 1950 A.D. We then used the calibration program OxCal (http://www.rlaha.ox.ac.uk/O/oxcal.php) to transform radiocarbon years into ages A.D./B.C. and present ranges that have a probability >95% of including the date of formation.

Statistical analysis

Vegetation – To determine the distribution of mollusk communities with respect to vegetation structure, we first sorted stations into five vegetation categories based on survey data and aerial photographs. The categories were: freshwater swamp forest, freshwater marsh, and dwarf, transitional and fringing mangrove forest and for quantitative analyses these were assigned numeric designations of 1-5, respectively. The distinctiveness of the categories based on relative cover of species present in more than 5% of the sites was confirmed using non-metric multidimensional scaling ordination (NMDS) and analysis of similarity (among community types) employing the Bray-Curtis similarity metric (using PCORD and PRIMER/ANOSIM software). The NMDS ordinations were determined for one to 10 dimensions and final ordination was retained that contained the number of dimensions above which no appreciable loss of stress occurred. Plant species significantly influencing the five community types were identified using Dufrene & Legendre's (1997) Indicator Species Analysis, where taxa having an indicator value (based on relative abundance and frequency among sites) above 40% of perfect indication ($P<0.05$) were considered reliable indicators.

Mapping - Using the spatial modeling and analysis (V2.0) module in Arcview GIS 3.2 ® (ESRI, CA), we mapped the distribution of vegetation community types, soil depth, peat depth and salinity. To interpolate between points, we used the Inverse Distance Weighted (IDW) method (McCune & Mefford, 1999), which weights the value of each point by the distance that point is from the cell being analyzed and then averages the values. The output grid cell size was 10 meters and the number of neighbors was 3 points.

Calibration - A transfer function was developed based on the relationships of modern mollusks to vegetation type and salinity to calibrate the mollusk assemblages in the sediment cores. The transfer function was developed using the weighted-averaging regression/calibration program in the software C2 ® (Juggins, 2003). This procedure assumes that the distribution of each species can be characterized by an optimum, defined by where abundances are greatest, and a tolerance, defined by the range of appearance along a gradient. The value of an environmental variable can then be calculated for a sample from an unknown environment, using the average of the optima of the species present, weighted by their abundances and, possibly, tolerances. Weighted-averaging regression/calibration performed in this manner requires the response gradient to be continuous and linear. While this was directly the case for salinity, we also used this method to predict vegetation community type from mollusk composition, as the community types were always arranged in the indicated sequence (forest-freshwater marsh-dwarf mangroves-transitional mangroves-fringing mangroves) and were suspected to have been so in the past.

Using the weighted-averaging program, we estimated the salinity (ppt) and vegetation optimum (using the 1-5 scale resulting from the NMDS) and tolerance for each mollusk species as the average among sites in which the species occurred. Salinity values were log transformed prior to analysis to fit a normal distribution. Because the mollusk species had unequal occurrences, we followed the recommendation of Birks et al. (1990) and used the number of occurrences to adjust the tolerance assigned to each species. When tolerances were incorporated into the model, mollusk species with narrow distributions along the gradient were weighted more heavily than species with broadly dispersed or erratic distributions. We used classical regression (Birks et al., 1990) to eliminate shrinkage in the range of inferred values, because it resulted in the most

evenly distributed residuals. We estimated the salinity and vegetation type at each site by randomly selecting samples from the same dataset (bootstrapping with replacement) and predicting values based on the remaining sites. The resulting estimates for each station were then plotted against observed values, reporting the R^2 of the relationship and root-mean squared error of prediction (RMSE). Residuals from this model were plotted against observed values to detect trends in estimation precision.

The model was then applied to predict the vegetation type and salinity from the relative abundances of mollusk species present in each bulk sediment subsample. Fractional values from vegetation type predictions were rounded to the next highest index value. Age-models from dated cores from the same subunit in the nearest basin were used to estimate the age range for each mollusk sample from undated cores. Then, for presentation purposes, mollusk-based vegetation type and salinity predictions were averaged within each of the three stratigraphic zones present in most cores. Predictions for each of these units were mapped using the same approach as for the environmental variables, as described above.

Results

Distribution of modern communities

Vegetation – Through multivariate community analyses, we were able to confirm the distinctiveness of the five major plant community types suggested through prior analysis of aerial photographs and survey data (see Gaiser et al., 2004). Based on relative cover 45 of the

most abundant of the 84 total plant species found in the study area, the ANOSIM comparison found a global R of 0.48 ($P<0.01$) for all combinations suggesting a high degree of compositional distinctiveness among all community types. Compositional differences within freshwater units (freshwater swamp forest and freshwater marsh) and interior mangrove units (dwarf and transitional) were less ($R = 0.2$ and 0.3, $P<0.05$, respectively) than differences between freshwater and mangrove units (mean $R = 0.4$, $P<0.01$), and the fringing mangrove forest was highly distinguishable from all other units (mean $R = 0.8$, $P<0.001$). A two-dimensional NMDS ordination (stress = 0.14) of the same data clearly shows this separation of freshwater and marine units (effectuated by the L-31E canal), and the general west-east gradient of composition from the interior to the coast (Fig. 2). Communities within the freshwater and brackish communities were further distinguished from each other by canopy height ($P<0.0001$ for all comparisons). Plant species significantly associated with each community type were: (1) in the freshwater swamp forest, *Boehmeria cylindrica* (L.) (false nettle), *Casuarina equisetifolia* (Australian pine), *Conocarpus erectus* L. (buttonwood), *Myrica cerifera* (L.) (wax myrtle), *Proserpinaca palustris* L. (marsh mermaidweed), *Psilotum nudum* (L.) (whisk fern), *Rhabdadenia biflora* (Jacq.) Mull. Arg. (mangrovevine), *Schinus terebinthifolius* (Brazilian pepper) and *Thelypteris kunthii* (Desv.) Morton (southern shield fern), (2) in the freshwater marsh, *Cladium jamaicense* Crantz (sawgrass), *Juncus roemerianus* Scheele (black rush) and *Typha domingensis* Pers. (cattail), (3) in the dwarf mangrove forest, *Laguncularia racemosa* (L.) Gaertn. (white mangrove), *Rhizophora mangle* L. (red mangrove) and *Rhynchospora microcarpa* Baldw. ex Gray. (southern beaksedge), and (4) in the transitional forest, *Acrostichum aureum* L. (leather fern) and *Avicennia germinans* L. (black mangrove). Unit 5 (fringing mangrove forest) had no species that alone defined the community but the three mangrove species (*Rhizophora*

mangle, Laguncularia racemosa and *Avicennia germinans*) together defined this unit. Though the coastward sequence of vegetation zones was consistent among sub-basins, there was variation in the breadth of each zone along the 7 km study area (Fig 3a). Further, we acknowledge that vegetation units are defined here very broadly to simplify linkages to mollusk community patterns. Additional distinct community types occur within these units, most notably including a densely vegetated, heavily canopied mangrove forest growing in historic drainages that meander through adjoining units and forests occupying tree islands that punctuate all units of the landscape. Vegetation canopy height was significantly higher in the freshwater swamp forest and transitional and fringing mangroves than in the freshwater marsh and dwarf mangrove community ($P<0.0001$; Fig. 3b).

Soils – Soil depth varied within the BBCW, being significantly deeper in the fringing mangrove forest than other units (126 vs. mean 104 cm, respectively). Areas of shallow soil coincided with areas of freshwater graminoid marsh, while deeper soils coincided with areas of coastal mangrove fringe forest. All of the sediment cores contained an upper heavily rooted peat underlain by compact marl. The contact between these layers was consistently abrupt and clearly defined. A basal layer of organic soil occurred beneath the marl layer in several cores taken from the fringing forest along the coastline. The upper peat layer was deepest in the fringing mangroves and gradually became shallower toward the interior freshwater marsh (66 vs 12 cm, respectively; Table 1, Figs. 4 a, b).

Salinity – Porewater salinity throughout the BBCW was in the fresh to brackish range at the time of sampling (1.6 – 27.6; mean 11.3 ppt). Although the point measurements taken here do not

represent the average salinity of the site, strong west-east increase was observed in most of the sub-basins, with the L-31E clearly separating freshwater (salinity < 5 ppt) from marine (5-20 ppt) conditions throughout the system (Fig. 4c). Pockets of higher salinity were observed in the interior of basins 2, 4, 6, 8 and 9, west of the fringing mangrove forest.

Mollusks – Mollusk shells were found in surface sediments of 74% of the survey sites. At these sites, shell density ranged from 1 to 93 per sample (mean = 10.6). At a mean soil bulk density of 0.2 g cm^{-3} and a mean sampling volume of 113 cm^3, we observed 0.46 shells g^{-1} or an aerial density of 938 shells m^{-2}. Twenty mollusk taxa representing 19 genera were collected and identified from the surface material (Table 2). Four taxa were identified at the generic level because of limitations restricting more precise identification, e.g. lack of soft anatomy. Within these four cases there appeared to be at least two to three species of each genus present. Therefore, a total of 24-28 species of 19 genera were present within the samples. Of the 20 mollusk species identified, three were bivalves, 17 were gastropods and three were terrestrial (Table 2). The dominant taxa found throughout the modern surface samples, represented by the highest number of occurrences, were *Littoridinops* spp., *Melanoides tuberculata*, *Cyrenoida floridana*, *Cerithidea costata,* and *Polymesoda maritime* (Table 2).

The weighted averaging (WA) salinity and vegetation type optima and tolerances (ppt) of 15 of the 20 species found in the 13 sub-basins showed a range of preferences (Table 2). Five of the 20 species were not included in the inference models and calculations due to inadequate representation in either the modern samples or sediments. Four mollusk species preferred freshwater to slightly brackish conditions: *Planorbella duryi, Physella cubensis, Planorbella*

scalaris, and Littoridinops spp, having salinity optima ranging from 1.94 (ppt) – 8.29 (ppt) (Table 2). The remaining 11 species had higher salinity optima (11.0 – 20.7 ppt) indicative of intertidal to marine conditions, including *Melanoides tuberculata*, *Polugira cereolus, Succinea barberi*, *Cyrenoida floridana*, *Daedalochila uvulifera*, unknown sp.1, *Melampus* spp., *Anomalocardia auberiana*, *Truncatella* spp., *Cerithidea costata*, and *Polymesoda maritime*.

The WA vegetation type optima suggested that three of the four freshwater taxa (*Planorbella duryi, Physella cubensis,* and *Planorbella scalaris*) prefer the freshwater swamp forest, while *Littiridinops spp*. preferred the freshwater graminoid marsh. Of the taxa preferring higher salinities, *Melanoides tuberculata*, *Cyrenoida floridana*, *Daedalochila uvulifera*, *Melampus* spp., *Anomalocardia auberiana*, and *Cerithidea costata* preferred the dwarf mangrove forest. The vegetation type optima of the five remaining species were, transitional mangrove forest (*Polygira cereolus*, uknown sp.1, and *Polymesoda maritime)* and coastal mangrove forest (*Succinea barberi* and *Truncatella* spp.; Table 2).

Weighted averaging regression models were used to test the strength of the relationship of mollusk species composition to salinity and vegetation type (Fig. 5a,b). Mollusk species composition was found to provide reliable predictions of salinity and vegetation type ($R^2 = 0.79$ and 0.67, respectively). Predictions for salinity were within 3.8 ppt and vegetation type within 1 unit, according to the predicted RMSE. We found no pattern in the relationship of model residuals with observed values for either parameter.

Core descriptions and chronology

Descriptions – The 10 dated cores had similar profiles to those obtained in the more extensive soil auger survey, having three or more stratigraphically distinct layers (Fig. 6). With the exception of core 7B, each had an upper dark brown/black, heavily rooted detrital mud surface layer (Munsell color 10YR 2/2, 5/2, 3/2) with a bulk density ranging from 0.03-0.1 g cm^{-3}, containing 50-85 % organic peat (mean 68 +/- 12 %). This layer was shallow (0-4 cm) in the freshwater forest and marsh, deeper in the dwarf mangrove forest (4-12 cm) and deepest in the transitional and fringing forest (18-42 cm). An abrupt transition was observed between this layer and a subsurface compact dark gray muck (Munsell color 10YR 4/1, 4/2) that also contained medium-sized roots and occasional darker colored compact organic masses. The lighter material was mostly marl with a bulk density of 0.09-0.45 g $cm^{-3}$and ranged from 8-41 % organic (mean 14 +/- 9 %) with a mean carbonate content of 51-86 %. The base of this layer was less sharply defined than the upper contact and, in most cores, graded into a hard, compact light gray/tan marl containing very fine roots and occasional small clumps of compact dark brown/black organic material (Munsell color 10YR 8/1, 8/2 with clumps of 10YR 2/1,). This basal layer had a bulk density of 0.3-0.9 g cm^{-3}, an organic content of 8-14 % (10 +/- 2 %) and carbonate content ranging from 70-90 %. Cores were driven to bedrock so this layer often contained chunks of limestone at the base, which were removed prior to analysis.

Chronology – The five cores from the transitional and fringing mangrove forest (9F, 7D, 7G, 7F and 2F) all had relatively smooth ^{210}Pb activity profiles, with unsupported ^{210}Pb extending to a depth of 25 – 50 cm (Fig. 7). Age-depth models (Fig. 7) show similar accumulation rates among

sites between ~ 1960 and the present, averaging 0.06 +/- 0.03 g cm^{-2} yr^{-1} (giving a mean vertical peat accretion rate of 0.3 cm yr^{-1}). Prior to 1960, the average accumulation rate in these cores averaged 0.04 +/- 0.03 g cm^{-2} yr^{-1}, significantly less than the modern period ($P<0.01$). Three cores from the freshwater marsh (10B, 1B and 1C) show an abrupt drop in unsupported ^{210}Pb within the upper 10 cm of sediment and the dating did not extend past the 1900's. Core 1C from the dwarf mangrove forest was intermediate between the two above categories; the profile for unsupported ^{210}Pb was relatively short (ending at 12 cm) but less abrupt, and the resulting chronology extends further back in time. The average accumulation rate from ^{210}Pb in these five cores was 0.03 +/- 0.02 g cm^{-2} yr^{-1}. Core 7B did not appear to reach supported (background) values, and was truncated below 27 cm by bedrock; the chronology therefore, was unreliable and not incorporated in analyses. In the remaining cores, the ^{210}Pb estimated age of the base of the upper peat layer ranged from 1946 to 1985 (mean = 1967) while that of the upper boundary of the underlying marl ranged from 1930 to 1966 (mean = 1944; Fig. 6). Extending the marl accumulation rates (0.03 – 0.04 g cm^{-2} yr^{-1}) beyond the period of measure provides an indication of the timing of the deeper transition in the cores, which ranges from 1705 to 1860 A.D.

The age of basal materials from the 5 cores analyzed for ^{14}C show that soil accumulation began earlier in the coastal fringe (900-2990 YBP) compared to the dwarf mangrove swamp (820 YBP) and freshwater marsh (310 YBP). We note that the older dates were from the bulk marl soils beneath the coastal peat (rather than plant fragments) and may, therefore, be influenced by older carbonates. Vertical accretion rates for these marl-dominated soils were calculated based on the amount of material accumulated between the ^{210}Pb date of the upper horizon of zone 2 and the

depth of the ^{14}C dated basal soil. Accretion rates range from 0.2 cm yr^{-1} in the coastal fringe to 0.02 cm yr^{-1} in the freshwater marsh and averaged 0.08 cm yr^{-1} among sites.

Paleoecological inferences from mollusks

Mollusk shells were found in all of the core samples, with densities ranging from 1-505 per sample (mean = 17.6) and 0.02-8.1 shells g^{-1} dry weight. Sediments contained 17 of the 20 taxa identified in the surface samples (*Melongena corona, Neritina virginea* and *Geukensia demissa granosissima* were not found in the sediments*)* and two taxa*, Pomacea paludosa* and *Haminoea elegans,* that were not represented by individuals in the surface samples. The dominant taxa found in the sediments, represented by the highest number of occurrences, were *Littoridinops* spp. and *Physella cubensis*.

Relative abundances of mollusk taxa differed among the three soil zones (Table 2). Zone 1 was dominated by *Littoridinops* spp. with subdominants *Physella cubensis* and *Cyrenioda floridana*. Zone 1 was also the only layer to contain *Melanoides tuberculata*, *Anomalocardia auberiana*, *Pomacea paludosa* and *Haminoea elegans*. Zone 2 contained greater abundances of *Littorindinops* spp. and *P. cubensis* than zone 1 and also contained *Planorbella duryi* and P. *scalaris* which were not found in the upper zone. Zone 3 was also dominated by *Littorindinops* spp. and had greater abundances of *P. cubensis*, *P. duryi* and *P. scalaris* than the upper 2 zones. *Melampus* spp., *C. floridana* and *A. auberiana* were conspicuously absent from zone 3 (Table 2).

Salinity inferences -- Contour maps of mollusk-inferred salinity for the coastal wetland system

show significant changes through the period of record (Fig. 8). Salinity inferences for the surface mollusk dataset used for calibration were mapped ("present", Fig. 8a) to visualize correspondence of the mollusk-based inferences with actual measured values (mapped in Fig. 4c). Patterns are generally similar with salinity decreasing shoreward with several small higher excursions to the interior. Average predicted salinity across the entire basin from the current mollusk assemblage was 13.2, while the sediment zones were significantly different with means of 6.9, 2.3 and 0.2 for zones 1, 2 and 3, respectively ($P<0.0001$; Fig. 8). Sediment zone 1, representing the last ~30-70 years shows a more abrupt interior-ward gradient of decreasing salinity with higher values isolated to the coastal fringe and small interior pockets in subunits 1, 7 and 9 (Fig. 10 a). Zone 2, representing the preceding 100-250 years of accumulation, shows mollusk-predicted salinity values ranged from 0-10 ppt, with one small pocket of higher values in the interior of subunit 1 (Fig. 8 b). Most of the coastal wetland unit could be classified as freshwater to slightly brackish (<5 ppt). All predictions for zone 3 were below 5 ppt (Fig. 8 c), indicating freshwater conditions persisted throughout the entire Biscayne Coastal Wetlands between the time that soils began accumulating and the 1700-1800's.

Vegetation inferences – Mollusk-based vegetation type predictions mapped for the surface community and sediment zones 1, 2 and 3 also show large magnitude changes over the period of record (Fig. 9). Contour maps show the high degree of correspondence between mollusk-based vegetation type predictions for surface assemblages (Fig 9a, "present") and actual measured vegetation types (Fig 3 a). Average predicted vegetation type was significantly different among the three sediment zones, with means of 3.1 (dwarf mangrove forest), 1.4 (freshwater marsh) and 1.1 (freshwater swamp forest) for zones 1, 2 and 3, respectively ($P<0.0001$). Zone 1 shows a

similar east-west zonation of vegetation types as depicted in the modern vegetation maps, with fringing and transitional mangrove forest lining the coastline, dwarf mangrove to the interior and freshwater marsh and swamp forests along the western boundary. There is notably less fringing mangrove forest predicted for zone 1 than measured in the vegetation survey (Fig. 9 a) or predicted from the modern mollusk community. The distribution of vegetation types during the time period encapsulated by zone 2 indicates a lack of distinct zonation with most of the BBCW being occupied by freshwater marsh and swamp forest (Fig. 9 b). A few small areas of subunits 1 and 2 appear to have been colonized by mangroves during this time. By the time interval represented by zone 1, the transitional mangrove forest had expanded 52 times its size in zone 2, and the dwarf and fringing forests had increased in area by a factor of 6 and 21, respectively. During the same interval, 85 and 59 percent of the freshwater swamp forest and marsh were lost. Inferences for Zone 3 suggest that the entire BBCW was freshwater marsh or forest, with forests occupying the majority of the unit and freshwater marshes being confined to the southernmost subunits (Fig. 9 c). Only 0.01 % of the area was occupied by mangroves (all dwarf forest).

Salt-water encroachment rates - Although fine-scale resolution of the temporal sequence of change was precluded due to the shallowness of the sediments and the need for bulk material to extract enough mollusks for analysis, we interpolated migration rates on a coarse scale by first determining the average longitude of the location of the freshwater swamp forest and marsh (the only two vegetation types present for the entire duration of record) for zones 1, 2, 3 and the present system. We then calculated the mean distance these communities shifted over the time interval elapsed between each sediment zone. The freshwater ecotones shifted interior-ward an average of 53 meters between zones 3 and 2, representing the long (300-3000 year) pre-

development period of deposition in this basin. The average pre-development encroachment rate was 0.14 m yr^{-1} (range, 0.02 to 0.27 m yr^{-1}). Between zones 2 (1700-1960) and 1 (1960-present), freshwater ecotones moved westward by an average of 450 meters, representing an encroachment rate of 3.1 m yr^{-1} (range 1.7 to 4.1 m yr^{-1}). While Zone 1 represents the past ~50 years and includes modern material, comparisons to surface assemblages show that encroachment continues in the contemporary community (Fig. 10).

Discussion

The rate of interior-ward migration of coastal ecotones along coastal South Florida has accelerated substantially in the past century. Rates of encroachment calculated in this study (2-4 m yr^{-1}) are one to two orders of magnitude faster in the past 60 years of record than in the previous history of the wetland unit. This rate is lower than that documented by Ross et al. (2000) who, by comparing community composition from a 1940 vegetation survey and aerial photographs with present data, found the boundary of mixed graminoid-mangrove and sawgrass communities in southeast Florida to have shifted inland by as much as 3.3 km, giving an encroachment rate of 55 m yr^{-1}. The difference may be due to the proximity of boundary canals in the two wetland units; in this study the L-31E canal is only ~600-900 m from the coast and prevents further westward encroachment while the area studied by Ross et al. (2000) is bounded 4 km to the west by the same canal. In the present study, the freshwater ecotone migrated 450 meters westward in the past 60 years and the <10% of original freshwater gramminoid marsh remaining is confined from further westward migration by agriculture and urban developments immediately adjacent to the study area. Also impacting westward movement of freshwater

marsh and forest components is the rapid invasion and expansion of exotic woody vegetation, including *Casuarina equisetifolia* and *Schinus terebinthifolius*, into areas that were formerly wetter.

The rapid loss of freshwater ecosystems from South Florida estuaries is due to a combination of rising sea-level and coastal water management practices. Rates of sea-level rise in South Florida, compiled for the Holocene by Wanless et al. (1994) from numerous stratigraphic studies, show relatively constant rates of approximately 0.4 mm yr^{-1} for the past 3000 years until the beginning of industrialization in the late 19th Century. The shallow and anastomosing geomorphology of the coastline in this region allowed for the development of mangroves, creating a sedimentary environment unique to North America, but similar to those of Caribbean island and continental coastlines. Unlike graminoid-dominated salt marshes that line much of the rest of the Atlantic coastline, mangrove communities have higher sedimentation rates that are commensurate with the moderate rates of sea-level rise characterizing the late Holocene. Accretion rates measured in this study of 0.3 and 0.08 cm yr^{-1}, based on ^{210}Pb and ^{14}C, respectively, were similar to the average calculated for mangrove ecosystems of the wider Caribbean region of 0.4 and 0.1 cm yr^{-1} (the discrepancy between historical and geological rates attributed to organic decomposition and sediment compaction; Parkinson et al., 1994). However, recent rates of sea-level rise calculated from the ~100 year tide gauge monitoring station in Key West show that the rate of sea level has increased by an order of magnitude over the period of record to 3-4 mm yr^{-1}, resulting in more than 30 cm increase in the last century (Maul & Martin 1993). Modern peat accretion rates suggest that mangroves in the BBCW are keeping up with the more rapid rate of sea-level rise and continuing to expand into marshland formerly occupied by a freshwater

gramminoid/sawgrass community. Ellison & Stoddart (1991) show that mangrove ecosystems can keep pace with rising sea level up to about 9 cm 100 yr^{-1}, which is less than the rate predicted for the next 100 years (10-12 cm 100 yr^{-1}, IPCC 1998). Ellison (1993) further showed that mangrove ecosystems quickly collapse in areas where this rate is greatly exceeded (i.e., Bermuda, where the local rate of sea-level rise exceeds 25 cm 100 yr^{-1}). An additional constraint on the ability of South Florida mangrove communities to colonize further under increasing rates of sea level rise is the occurrence of intermittent freezes, which are poorly tolerated by the dwarf mangrove communities (Ross et al., unpublished manuscript). Despite the low aboveground production of the dwarf forests, apparently in response to P-limitation on the carbonate soils of the interior coastal areas (Feller, 1995; Ross et al. 2003), belowground production is sufficient to build a significant peat soil layer (Fig. 4b), thereby increasing site productivity and affecting vegetation succession.

Freshwater marsh vegetation type from the Florida coastline is not only being lost as it is replaced by mangroves advancing with sea-level rise but also by salt-water encroachment exacerbated by water management practices. Prior to construction of the water conveyance system in South Dade in the early 1900's, freshwater flowed from the Everglades into Biscayne Bay through natural transverse glades. Freshwater delivery through these drainages was evidently substantial enough to maintain freshwater salinities throughout the BBCW. Mangroves were restricted to a peripheral fringe which appears on aerial photographs from the 1940's to have occupied a narrow band along the edge of the study unit, as well as along the mouths of the tidal creek outlets (Ross et al., 2000). Freshwater drainage in this basin began with the construction of small ditches (mosquito ditches) to drain water from expanding

agricultural land. Major canal construction began in the 1940's when the Princeton, Military and Mowry canals were dug as flood control canals, diverting most freshwater from the Everglades into focused discharges in Biscayne Bay. Finally, the L-31E canal was constructed in 1960 to connect the network of east-west drainage canals and combat saltwater intrusion further to the west. This canal network effectively eliminated the natural eastward flow of freshwater through this system and caused the tidal creeks to fill in with sediment, resulting eventually in the formation of prominent strand forest formations (Meeder et al., 2000). Patterns in the distribution of porewater salinity values are now driven by the underlying drainage template. Although we stress that the inferences presented here are based on point measurements rather than average values, the general pattern is clear. Freshwater is completely confined to the west of the L-31E drainage while higher salinities can develop in the interior of each basin where circulation is limited due to higher elevation berms on the east (resulting from storm deposits) and the south and north due to forest vegetation lining former drainages. Sawgrass meadows, once dominant along the coast, are now also confined to freshwater units west of the L-31E canal, being displaced by salt-tolerant *R. mangle.* It is notable that these sawgrass meadows were likely interspersed with woody vegetation, possibly in tree islands (which are reduced in number today), since the mollusk fauna in basal material contained more terrestrial taxa than modern sawgrass communities. However, the freshwater swamp forest habitat unit that prevailed through the majority of the 2000 yr history of the BBCW would have had a very different composition from the modern forest, which is now dominated by invasive *Casuarina equisetifolia* and *Schinus terebinthifolius.* Instead, surveys in this region conducted prior to the spread of these invasives (Teas et al., 1976) suggest that this forest was comprised of water-tolerant bayhead taxa, including *Conocarpus erectus* (buttonwood) and *Myrica cerifera* (wax

myrtle) and possibly, in drier areas of higher elevation, hammock/coastal hardwood taxa such as *Sabal palme*tto (Walter) Loddiges ex Schultes & Schultes (cabbage palm), *Bursera simaruba* (L.) Sarg. (gumbo-limbo) and *Metopium toxiferum* Krug & Urb. (poison wood).

Mollusks have been reliable indicators of paleoenvironments, particularly of sea-level rise and associated changes, in carbonate-rich, shallow-water coastlines and bays. They are diverse and abundant in estuarine/marine settings and preserve well in the low solute, high pH interstitial environment. Ross et al. (2001) found a similar assemblage of mollusks along a coastal transect in a nearby wetland, and found strong correspondence of assemblage composition with distance from the coastline. The high degree of variability in salinity in that study, however, precluded the estimation of salinity preferences for collected taxa. However, the placement of taxa along the coastal gradient was similar in the two studies, with *Physella cubensis* and *Planorbella* spp. being restricted to freshwater marshes, *Litterindinops* spp, *Polygira cereolus* and *Cyrenioda floridana* preferring the intermediate dwarf mangrove forest, and *Melampus* spp. and *Cerithidea* spp. being associated more closely with the marine coastline. We do, however, caution that the optima presented here are inferred from point (rather than mean) salinity measurements, so they should be used for relative rather than absolute quantitative purposes. In this way they are useful, however, as in Brewster-Wingard et al. (2001), who collected mollusks from a high density of sites in Florida Bay, and used strong associations with salinity to reliably elucidate increasing environmental variability (particularly in salinity) over the past 100 years in sediment cores. Salinity and temperature preferences are provided for 43 taxa, but only four taxa (*Melampus* spp., *Anomalocardia* auberiana, *Truncatella* spp. and *Melongena corona*) were also found in the present study. The low degree of overlap between the fauna collected by Brewster-

Wingard et al. (2001) from a shallow embayment and the coastal wetland studied here is expected; also that the four overlapping taxa had marine salinity optima in both studies. To our knowledge this is the first presentation of quantitative salinity and vegetation type preferences for many of these brackish-water species, and should provide a reliable guide for other mollusk-based ecological research in this region.

Conclusions

There is clear evidence from the mollusk record that salt-water is rapidly encroaching in the BBCW and this is eliminating the formerly expansive freshwater marsh ecosystem and associated natural tidal drainages. Mangroves are advancing inland at rates similar to those seen in other coastal Caribbean environments, and the pace of migration is only curtailed by artificial impediments such as canals, levees or developing urban and agricultural landscapes. Ross et al. (1991) compared vegetation distributions in aerial photographs from 1935 and 1991 from the lower Florida Keys and also found an increase in mangrove expanse of 33 percent over the 56 yr period. Along the Atlantic coastline, sea-level rise and other contributing factors have caused the loss of over 50% of tidal wetlands since the 1800's (Ellison, 1993), a process particularly severe in areas of low relief and high erosion (i.e., Louisiana's coastal wetlands, Childers & Day, 1990). These problems will only be exacerbated by the combined pressures of development and climate change. Active intervention is necessary which could include massive re-routing of freshwater drainages to re-establishing the natural tidal drainage through coastal wetlands and protecting land behind mangroves to allow areas for inland migration of existing freshwater and estuarine communities.

Acknowledgements

This work could not have been possible without the generous assistance of the staff of the Southeast Environmental Research Center (SERC), especially Christine Taylor, Alexander Leon, David Reed, David Jones and Jay Sah in the field and laboratory. We also thank Sarah Bellmund and Biscayne National Park for continued support of this project, Lynn Coultas for assistance in soil sampling and interpretation and Krish Jayachandran for soil characterization and analysis. Radiometric analyses were performed by Beta Analytic, Miami, FL (^{14}C) and Daniel Engstrom (^{210}Pb), who also helped with chronological interpretations. We thank Victor Monroy-Rivera, Gail Chmura and Joel Trexler for very thorough and helpful reviews of this manuscript. Funding was provided to SERC from the United States Department of the Interior, Everglades National Park. Additional support has been provided by the National Science Foundation through the Florida Coastal Everglades LTER program (DEB-9910214), Research Experiences for Undergraduates and FIU Undergraduate Mentoring in Environmental Biology Programs (DEB-0102832). This is SERC publication series contribution #xxx.

References

Abbott, R. T., 1954. American Seashells, 1st Edition. Van Norstrand Reinhold, New York, NY: 541 pp.

Appleby, P. G. & F. Oldfield, 1978. The calculation of lead-210 dates assuming a constant rate of supply of unsupported ^{210}Pb to the sediment. Catena 5: 1-8.

Binford, M. W., 1990. Calculation and uncertainty analysis of ^{210}Pb dates for PIRLA project lake sediment cores. Journal of Paleolimnology 3: 253-267.

Birks, H. J. B., J. M. Line, S. Juggins, A. C. Stevenson & C. J. F. Ter Braak, 1990. Diatoms and pH reconstruction. Philosophical Transactions of the Royal Society of London B. 327: 263-278.

Boyer, J. N., J. W. Fourqurean & R. D. Jones, 1999. Seasonal and long-term trends in water quality of Florida Bay (1989-97). Estuaries 22: 417-430.

Brewster-Wingard, G. L., J. R. Stone & C. W. Holmes, 2001. Molluscan faunal distribution in Florida Bay, past and present: An integration of down-core and modern data. In B. R. Wardlaw (ed.) Paleoecological Studies of South Florida. Bulletins of American Paleontology 361: 199-232.

Childers, D. L. & J. W. Day, 1990. The dilution and loss of wetland function with conversion to open water. Wetlands Ecology and Management 1: 1-9.

Church, J. A., J. M. Gregory, P. Huybrechts, M. Kuhn, K. Lambeck, M. T. Nhuan, D. Qin & P. L. Woodworth, 2001. Changes in sea level. Chapter 11 of the Intergovernmental Panel on Climate Change Third Assessment Report, Science Report, Cambridge University Press, Cambridge, UK: 638-689

Dufrene, M. & P. Legendre, 1997. Species assemblages and indicator species: the need for a flexible asymmetrical approach. Ecological Monographs 67: 345-366.

Eakins, J. D. & R. T. Morrison, 1978. A new procedure for the determination of lead-210 in lake and marine sediments. International Journal of Applied Radiation and Isotopes 29: 531-536.

Egler, F. E., 1952. Southeast saline Everglades vegetation, Florida, and its management. Vegetatio Acta Geobotanica 3: 213-265.

Ellison, J. & D. R. Stoddart, 1991. Mangrove ecosystem collapse during predicted sea-level rise: Holocene analogues and implications. Journal of Coastal Research 7: 151-165.

Feller, I. C., 1995. Effects of nutrient enrichment on growth and herbivory of dwarf red mangrove (Rhizophora mangle). Ecological Monographs 65: 477-505.

Gaiser, E. E., A. Wachnicka, P. Ruiz, F. Tobias & M. S. Ross, 2004. Diatom indicators of ecosystem change in coastal wetlands. In Bortone, S. (ed.), Estuarine Indicators. CRC Press, Boca Raton, FL: 127-144.

Intergovernmental Panel on Climate Change, 1998. The Regional Impacts of Climate Change: An Assessment of Vulnerability. Special Report of IPCC Working Group II. In Watson, R. T., M. C. Zinyowera & R. H. Moss (eds.), Intergovernmental Panel on Climate Change, Cambridge University Press, Cambridge, United Kingdom and New York, NY: 517 pp.

Juggins, S., 2003. C2 User guide: Software for ecological and palaeoecological data analysis and visualization. University of Newcastle, Newcastle upon Tyne, UK.

Leatherman, S. P., K. Zhang & B. C. Douglas, 2000. Sea level rise shown to drive coastal erosion. Eos (Transactions American Geophysical Union) 81: 55-57.

Maul, G. A. & D. M. Martin, 1993. Sea level rise at Key West, Florida, 1846-1992: America's longest instrument record? Geophysical Research Letters 20: 1955-1958.

McCune, B. & M. J. Mefford, 1999. Multivariate analysis of ecological data. Version 4.17. MJM Software. Gleneden Beach, OR.

Meeder, J. F., P. W. Harlem, M. S. Ross, E. E. Gaiser & R. Jaffe, 2000. Southern Biscayne Bay Watershed Historic Creek Characterization. Final Report to the South Florida Water Management District.

National Research Council ,1993. Managing wastewater in coastal urban areas. Washington DC: National Academy Press.

Nicholls, R. J., F. M. J. Hoozemans & M. Marchand, 1999. Increasing flood risk and wetland losses due to sea-level rise: regional and global analyses. Global Environmental Change, 9: S69-S87.

Park, R.A., M. S. Trehan, P. W. Mausel & R. C. Howe, 1989. Coastal wetlands in the twenty-first century: Profound alterations due to rising sea level. In Fisk, D. W. (ed.), Wetlands: Concerns and Successes. Proceedings of the American Water Resources Association, Tampa, FL, USA:.71-800.

Parkinson, R. W., R. D. DeLaune & J. R. White, 1994. Holocene sea-level rise and the fate of mangrove forests within the wider Caribbean region. Journal of Coastal Research 10: 1077-1086.

Ross, M. S., L. J. Flynn & J. J. O'Brien, 1991. Has 20th Century sea level rise caused the migration of Florida Keys plant communities? American Journal of Botany (Supplement) 78: 46.

Ross, M. S., J. F. Meeder, J. P. Sah, P. L. Ruiz & G. J. Telesnicki, 2000. The Southeast Saline Everglades revisited: a half-century of coastal vegetation change. Journal of Vegetation Science 11: 101-112.

Ross, M. S., E. E. Gaiser, J. F. Meeder & M. T. Lewin, 2001. Multi-taxon analysis of the "white zone", a common ecotonal feature of South Florida coastal wetlands. In Porter, J. & K. Porter (eds), The Everglades, Florida Bay, and Coral Reefs of the Florida Keys. CRC Press, Boca Raton, FL: 205-238.

Ross, M. S., J. F. Meeder, E. E. Gaiser, P. L. Ruiz, J. P. Sah, D. L. Reed, J. Walters, G. T. Telesnicki, A. Wachnicka, M. Jacobson, J. Alvord, M. Byrnes, C. Weekley, Z. D. Atlas, M. T. Lewin, B. Fry, & . Renshaw, 2003. The L-31E Surface Water Rediversion Pilot Project Final Report: Implementation, Results, and Recomendations. Report to South Florida Water Management District (SFWMD Contract C-12409).

Teas, H. J., H. R. Wanless & R. Chardon, 1976. Effects of man on the shore vegetation of Biscayne Bay. In Thorhaug, A. & A. Volker (ed.), Biscayne Bay: Past/Present/Future. University of Miami Sea Grant Special Report, Miami, FL: 133-157.

Thompson, F.G., 2002. An Identification Manual for the Freshwater Snails of Florida. [Online] http://www.flmnh.ufl.edu/natsci/malacology/fl-snail/snails1.htm.

Wanless, H. R., R. W. Parkinson & L. P. Tedesco, 1994. Sea level control on stability of Everglades Wetlands. In Davis S. M. & Ogden J. C. (eds.), Everglades: the Ecosystem and Its Restoration. St. Lucie Press, St. Lucie, FL: 199-222.

Figure legends:

Figure 1. Satellite image of Florida with inset aerial image of the Biscayne Bay Coastal Wetlands in 1990 showing the location of (a) sites used to survey vegetation, mollusks, salinity and soil characteristics, and (b) coring sites used for the paleoecological survey. The left panel also shows the numerical designation of wetland subunits (separated by east-west drainage ditches) while the right panel shows the major drainage canals in the region.

Figure 2. Non-metric multidimensional scaling ordination biplot of suvery sites based on compositional dissimilarity of vegetation communities, showing differentiation of the five vegetation type categories.

Figure 3. Contour maps generated from the vegetation survey showing the distribution of (a) community types and (b) mean canopy height across the Biscayne Bay Coastal Wetlands. Sampling locations are indicated on the corresponding aerial image (Fig. 1 a).

Figure 4. Contour maps generated from the soil survey showing the distribution of (a) soil depth, (b) depth of the upper peat layer in soil cores and (c) porewater salinity across the Biscayne Bay Coastal Wetlands. Sampling locations are indicated on the corresponding aerial image (Fig. 1 a).

Figure 5. Relationships between observed and mollusk-inferred values of (a) salinity and (b) vegetation type using classical weighted-averaging regression with tolerance down-weighting.

The root mean squared error of prediction based on bootstrapping with replacement within the survey dataset is provided.

Figure 6. Characterization of sediments in the chronologically calibrated cores, indicating the estimated ^{210}Pb date of material above and below the upper peat zone. Coring locations are depicted in Fig 1 b.

Figure 7. Age-depth models (upper panels) and associated ^{210} Pb activities (lower panels) for the 10 cores. The left panels show accumulation rates and activities for cores collected from the freshwater swamp forest, freshwater marsh and dwarf mangrove forest while the right panels show results from the transitional and fringing mangrove forest.

Figure 8. Contour maps of vegetation types based on weighted-averaging regression/calibration inferences from mollusk assemblage composition in surface material (present) and sediment zones 1, 2 and 3. Coring site locations are indicated.

Figure 9. Contour maps of salinity based on weighted-averaging regression/calibration inferences from mollusk assemblage composition in surface material (present) and sediment zones 1, 2 and 3. Coring site locations are indicated.

Figure 10. Area occupied by each vegetation type type and porewater salinity concentrations (with standard error bars) predicted by mollusk communities in surface soils (present) and sediment zones 1, 2 and 3.

Table 1. Means and standard errors () of soil depth, peat depth, vegetation canopy cover and salinity for each vegetation community type (with designated numeric reference categories).

Vegetation Type	Category	Soil Depth (cm)	Peat Depth (cm)	Canopy Height (m)	Salinity (ppt)
Freshwater Swamp Forest	1	93 (20)	24 (10)	5 (2)	2.2 (0.9)
Freshwater Marsh	2	118 (13)	12 (2)	2 (1)	4.9 (4.3)
Dwarf Mangrove Forest	3	97 (21)	26 (18)	2 (1)	9.0 (8.0)
Transitional Mangrove Forest	4	108 (19)	41 (16)	5 (2)	16.0 (6.7)
Fringing Mangrove Forest	5	126 (14)	66 (27)	9 (2)	17.6 (2.0)

Table 2. Number of occurrences, maximum relative abundances, and weighted-averaging (WA) salinity (ppt) and vegetation type optima and tolerances () of mollusks collected from surface sediments in the Biscayne Bay Coastal Wetlands. Relative abundances in zones 1, 2 and 3 of the sediment cores are also provided. Species are listed in increasing order of estimated WA salinity optima.

Taxon	**No. Occ. Surface**	**Max Rel. Abd. Surface**	**WA Salinity Opt. (Tol.)**	**WA Vegetation Opt. (Tol.)**	**Rel. Abd. Zone 1**	**Rel. Abd. Zone 2**	**Rel. Abd. Zone 3**
Planorbella duryi (Weatherby)	3	0.14	1.94 (0.42)	1.00 (1.11)	0	0.01	0.01
Physella cubensis (Pfeiffer)	15	0.67	2.09 (0.46)	1.39 (0.58)	0.09	0.15	0.2
Planorbella scalaris (Jay)	2	0.14	2.33 (0.12)	1.35 (0.71)	0	0.01	0.03
Littorindinops spp.	41	1	8.29 (7.96)	2.35 (1.29)	0.57	0.73	0.6
Melanoides tuberculata (Müller)	32	1	11.01 (8.45)	3.15 (1.02)	0.01	0	0
Polygira cereolus	2	0.37	12.82 (8.14)	4.71 (2.83)	0.01	0.01	0.02
Succinea barberi	2	0.11	13.65 (4.84)	5.00 (1.11)	0	0.01	0.02
Cyrenioda floridana (Dall)	35	0.93	15.60 (7.78)	3.60 (1.02)	0.09	0.01	0

Daedalochila uvulifera	2	0.17	16.17 (4.84)	3.00 (1.11)	0	0.01	0.01
Unknown sp. 1	9	0.57	16.26 (5.30)	4.27 (0.87)	0.04	0	0
Melampus spp.	13	0.88	16.54 (6.52)	3.63 (0.84)	0.04	0.01	0
Anomalocardia auberiana (Orbigny)	4	0.05	18.55 (5.69)	3.87 (1.19)	0.01	0	0
Truncatella spp.	4	0.58	18.77 (3.29)	5.00 (1.11)	0.06	0.1	0.08
Cerithidea costata (da Costa)	23	0.77	20.36 (5.08)	3.79 (0.88)	0.05	0.02	0.01
Polymesoda maritima (Orbigny)	23	0.85	20.73 (3.64)	4.09 (0.95)	0.01	0.1	0.01
Melongena corona (Gmelin)	1	0.03			0	0	0
Geukensia demissa granosissima (Sowerby)	4	0.01			0	0	0
Pomacea paludosa (Say)	0	0			0.01	0	0
Haminoea elegans (Gray)	0	0			0.01	0	0
Neritina virginea (Linné)	1	0.01			0	0	0

Table 3. Depth and identity of samples from the Biscayne Coastal Wetlands analyzed for radiocarbon by Beta Analytic, Miami, FL. Samples were analyzed by Accelerated Mass Spectrometry (AMS) or by extended counting on a scintillation spectrometer.

Core	**Depth below surface (cm)**	**Conventional ^{14}C age ***	**Calibrated ^{14}C age ****	**Analysis/Sample type**	**Beta ID**
7D	50-54	1750 +/- 40	230-350 A.D.	AMS/bulk organic	Beta-194070
1B	60-64	310 +/- 40	1460-1660 A.D.	AMS/plant fragments	Beta-194071
1C	42-44	820 +/- 40	1150-1280 A.D.	AMS/plant fragments	Beta-194072
7F	96-98	900 +/- 40	1030-1220 A.D.	AMS/plant fragments	Beta-194073
2F	88-90	2990 +/- 60	1390-1110 B.C.	Extended/peat	Beta-194074

*Dates are reported in RCYBP (radiocarbon years before present, 'present' = 1950 A.D.).

**Dates calibrated using OxCal ® software.

Figure 1

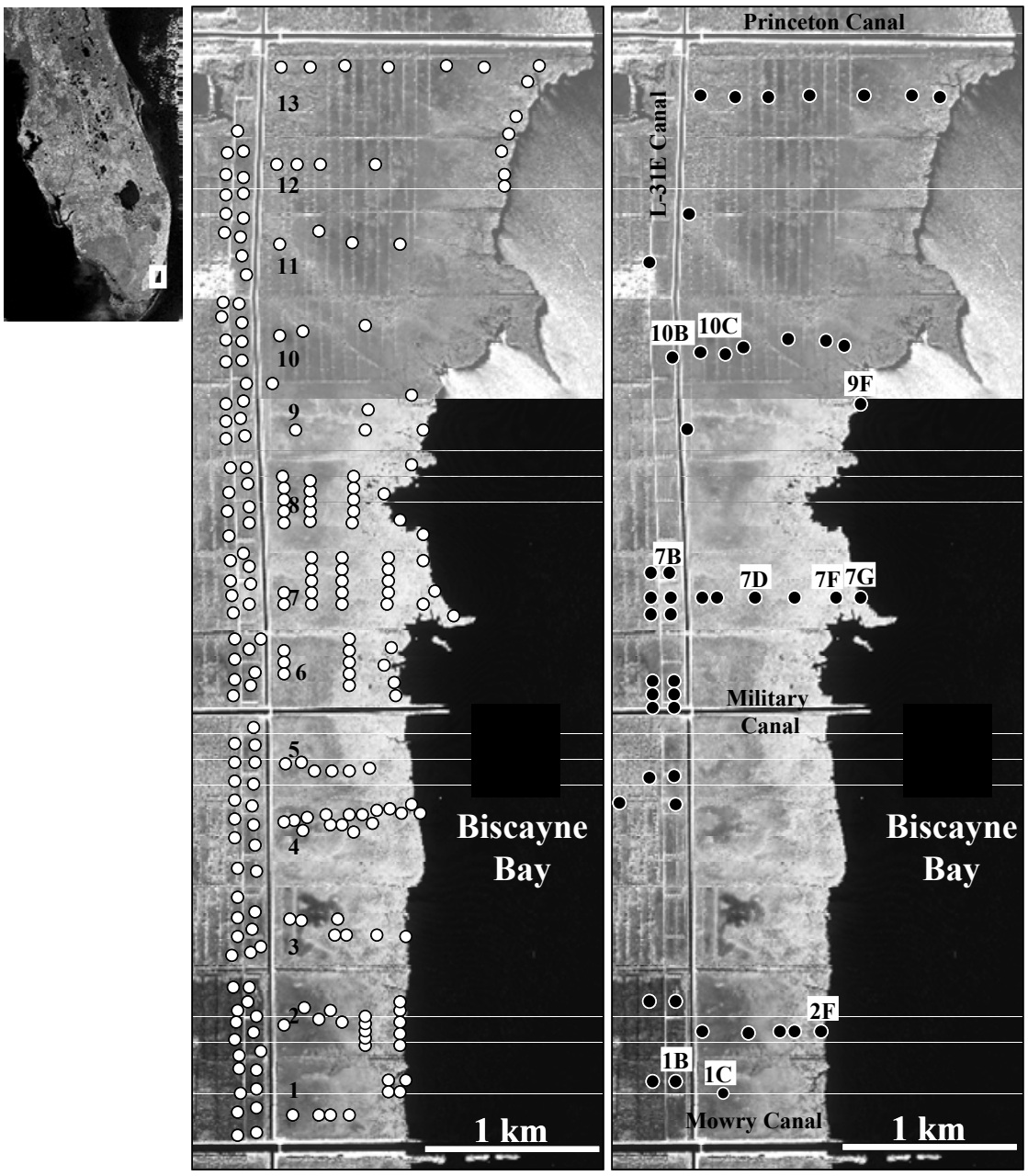
A. Survey Sites
B. Coring Sites
13
12
11
10
9
8
7
6
5
4
3
2
1
Biscayne Bay
1 km
Princeton Canal
L-31E Canal
10B
10C
9F
7B
7D
7F
7G
Military Canal
Biscayne Bay
2F
1B
1C
Mowry Canal
1 km

Figure 2

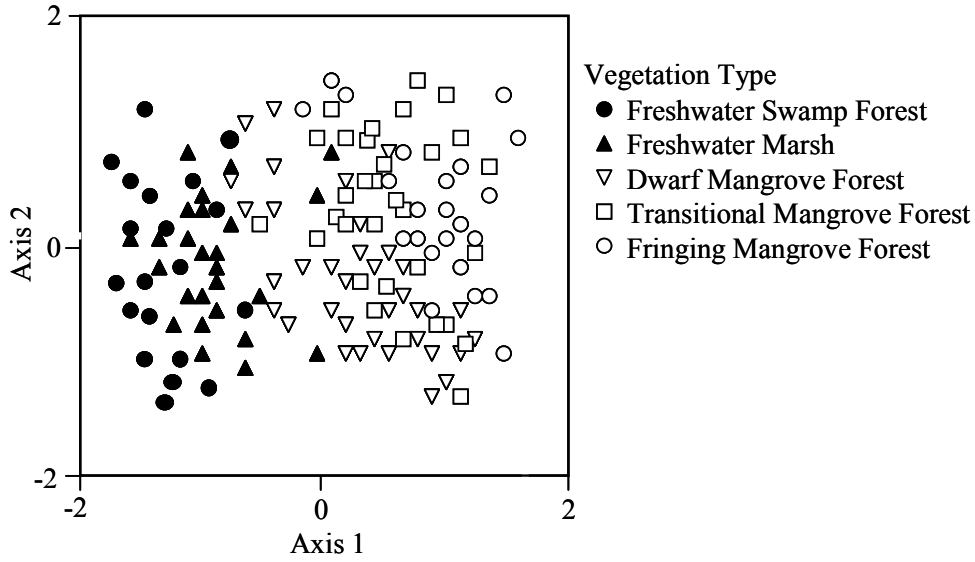
2
0
-2
Axis 2
-2
0
2
Axis 1
Vegetation Type
Freshwater Swamp Forest
Freshwater Marsh
Dwarf Mangrove Forest
Transitional Mangrove Forest
Fringing Mangrove Forest

Figure 3

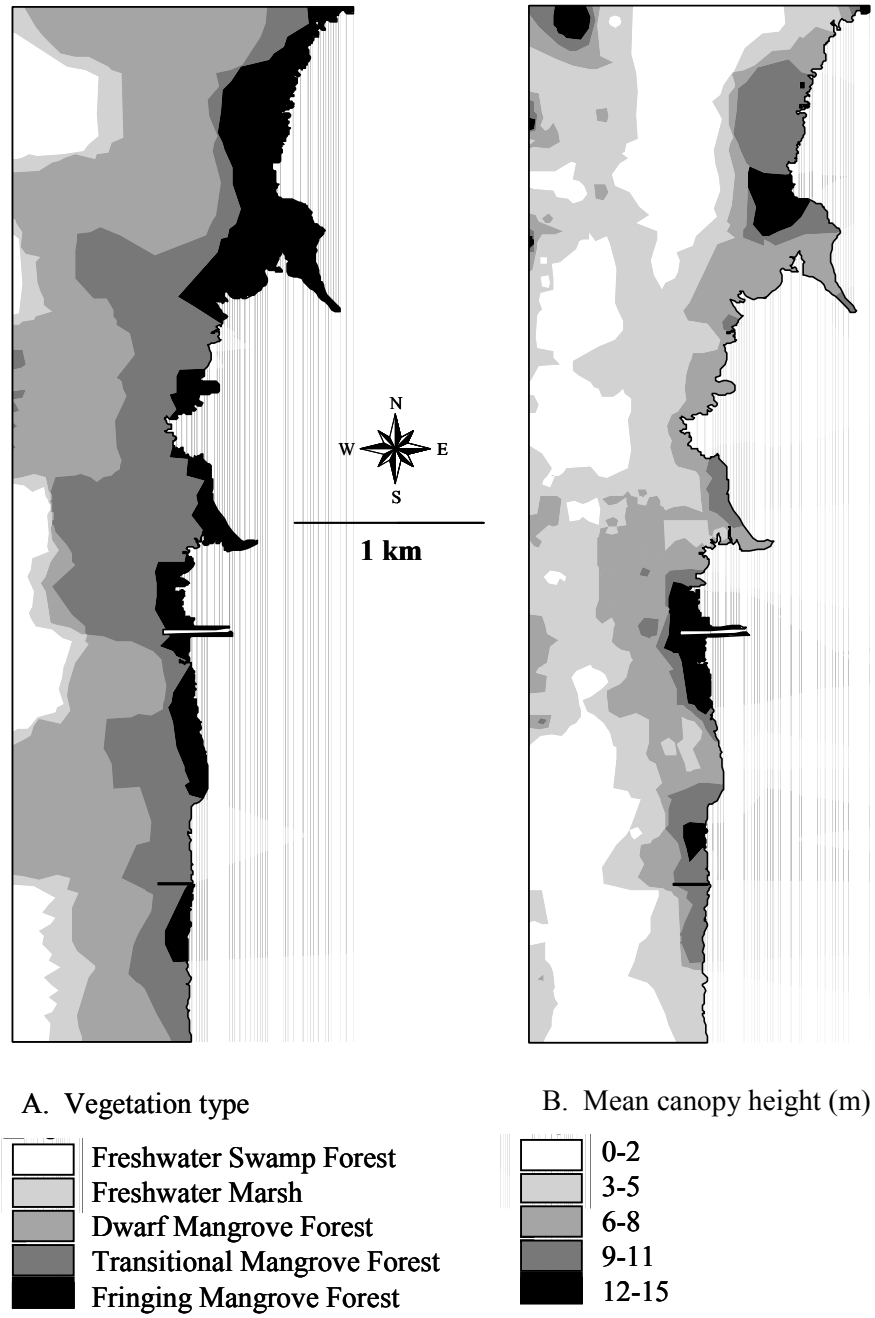
N
W
E
S
1 km
A. Vegetation type
Freshwater Swamp Forest
Freshwater Marsh
Dwarf Mangrove Forest
Transitional Mangrove Forest
Fringing Mangrove Forest
B. Mean canopy height (m)
0-2
3-5
6-8
9-11
12-15

Figure 4

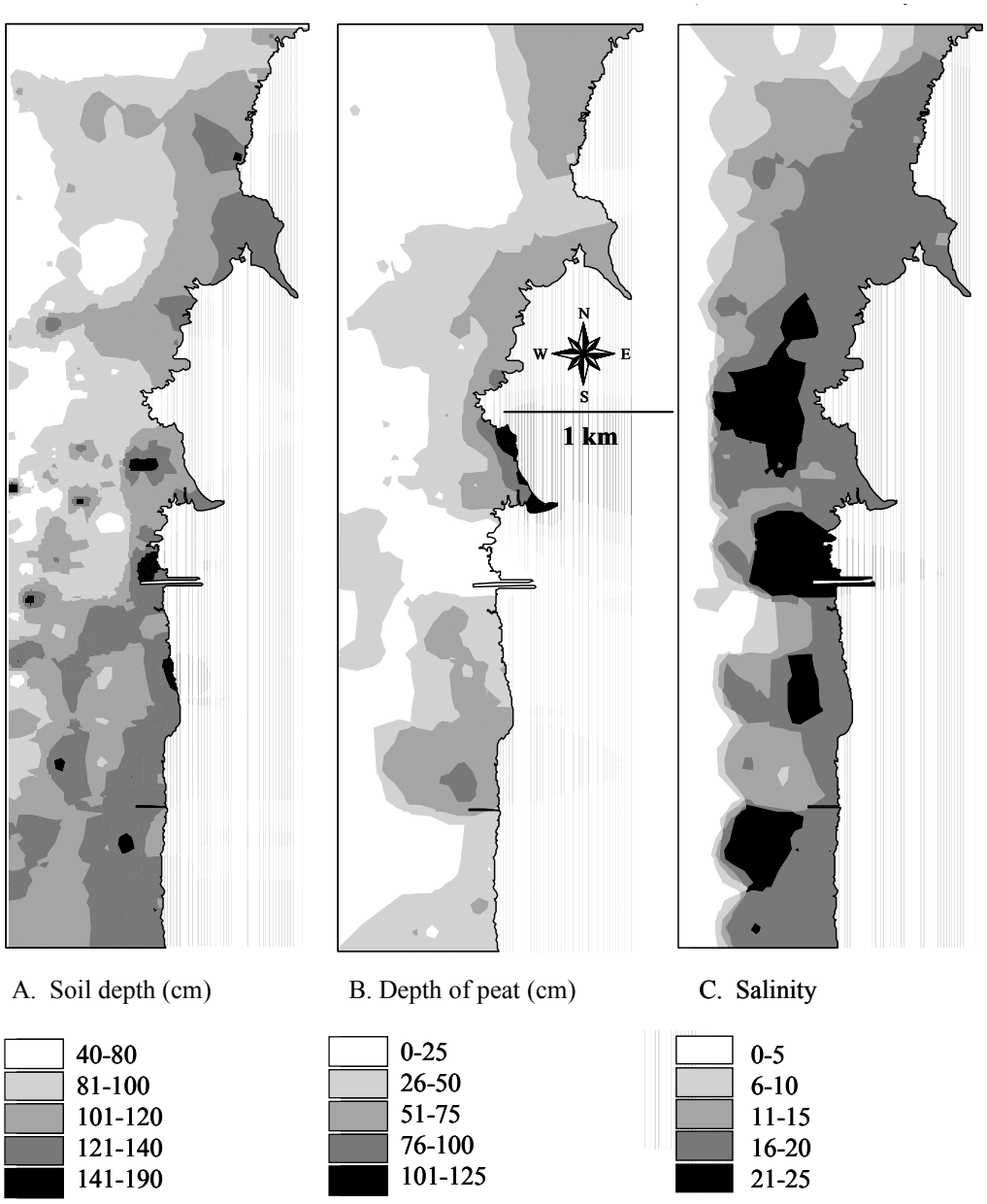
N
W
E
S
1 km
A. Soil depth (cm)
40-80
81-100
101-120
121-140
141-190
B. Depth of peat (cm)
0-25
26-50
51-75
76-100
101-125
C. Salinity
0-5
6-10
11-15
16-20
21-25

Figure 5

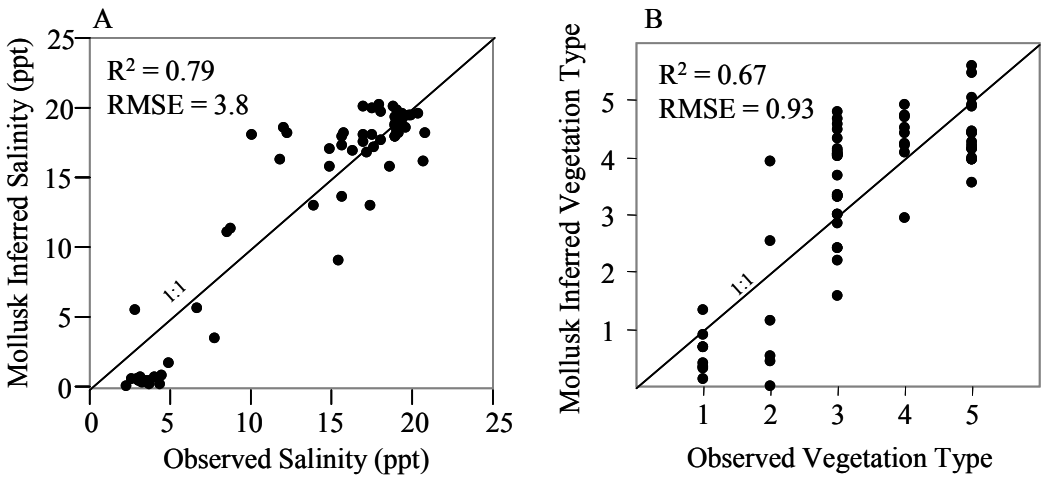
A
R² = 0.79
RMSE = 3.8
1:1
Mollusk Inferred Salinity (ppt)
Observed Salinity (ppt)
0
5
10
15
20
25
B
R² = 0.67
RMSE = 0.93
1:1
Mollusk Inferred Vegetation Type
Observed Vegetation Type
1
2
3
4
5

Figure 6

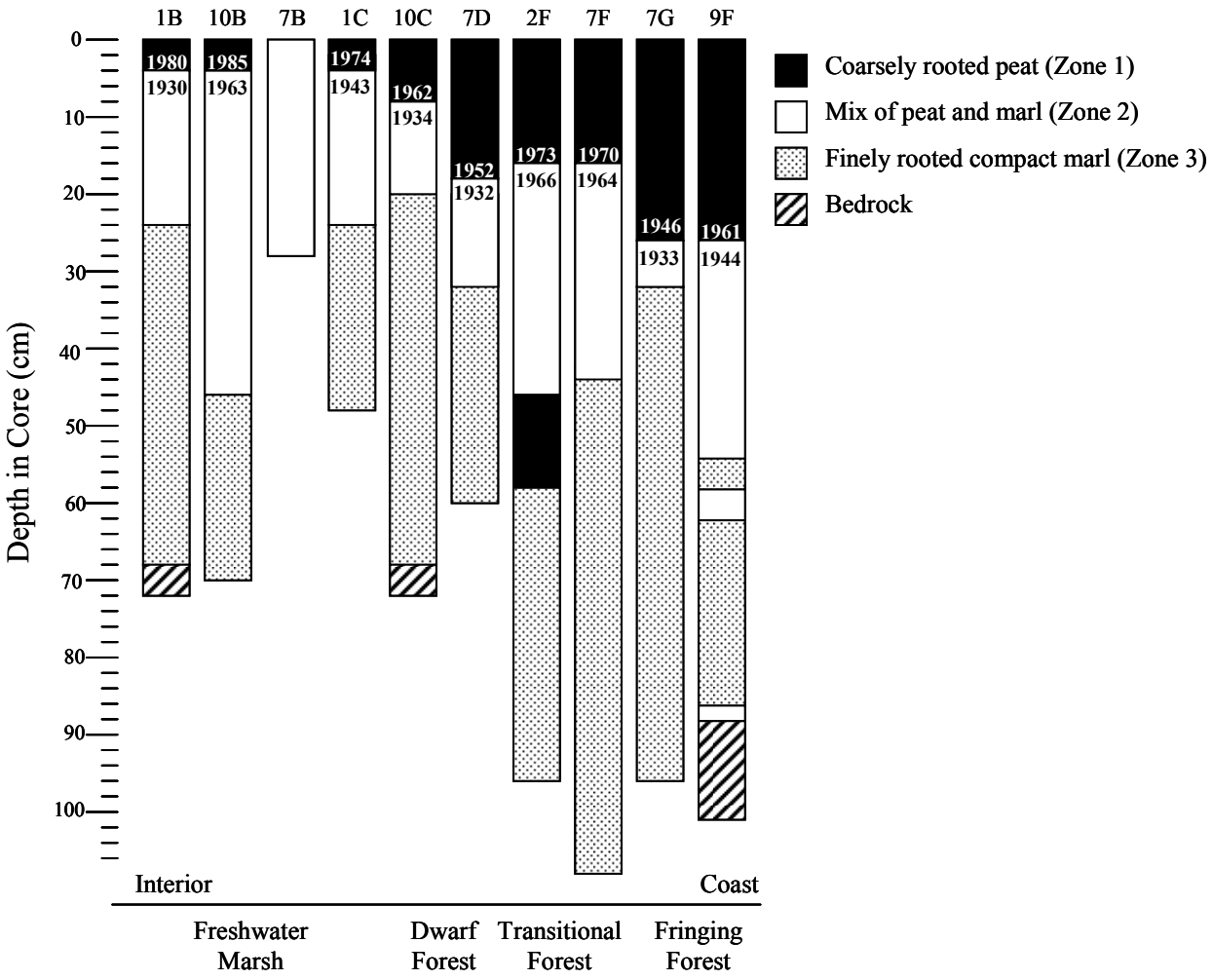
1B
10B
7B
1C
10C
7D
2F
7F
7G
9F
1980
1930
1985
1963
1974
1943
1962
1934
1952
1932
1973
1966
1970
1964
1946
1933
1961
1944
Depth in Core (cm)
0
10
20
30
40
50
60
70
80
90
100
Interior
Coast
Freshwater Marsh
Dwarf Forest
Transitional Forest
Fringing Forest
Coarsely rooted peat (Zone 1)
Mix of peat and marl (Zone 2)
Finely rooted compact marl (Zone 3)
Bedrock

Figure 7

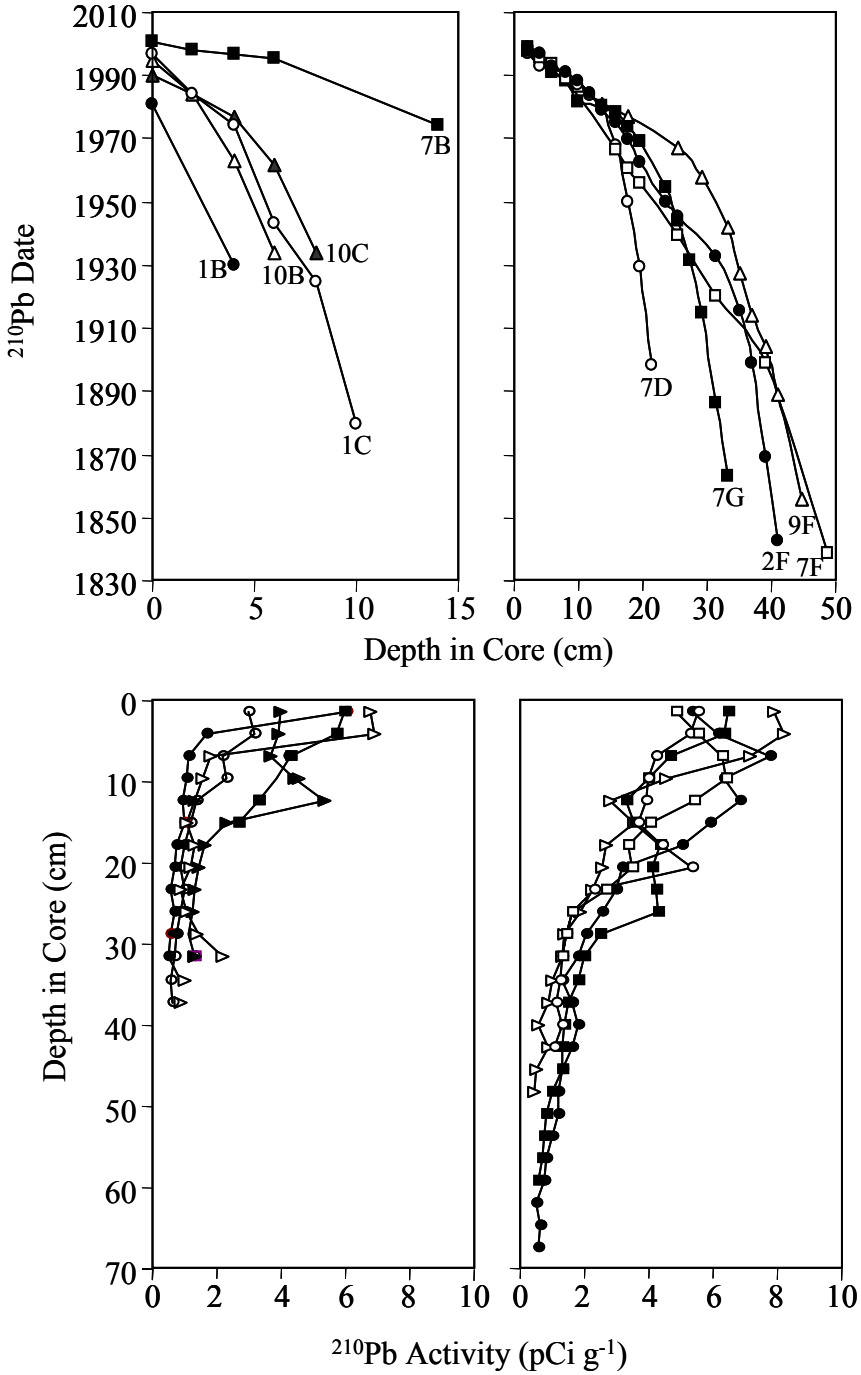
2010
1990
1970
1950
1930
1910
1890
1870
1850
1830
^{210}Pb Date
7B
10C
1B
10B
1C
7D
7G
9F
2F
7F
0
5
10
15
20
30
40
50
Depth in Core (cm)
Depth in Core (cm)
60
70
2
4
6
8
^{210}Pb Activity (pCi g^{-1})

Figure 8

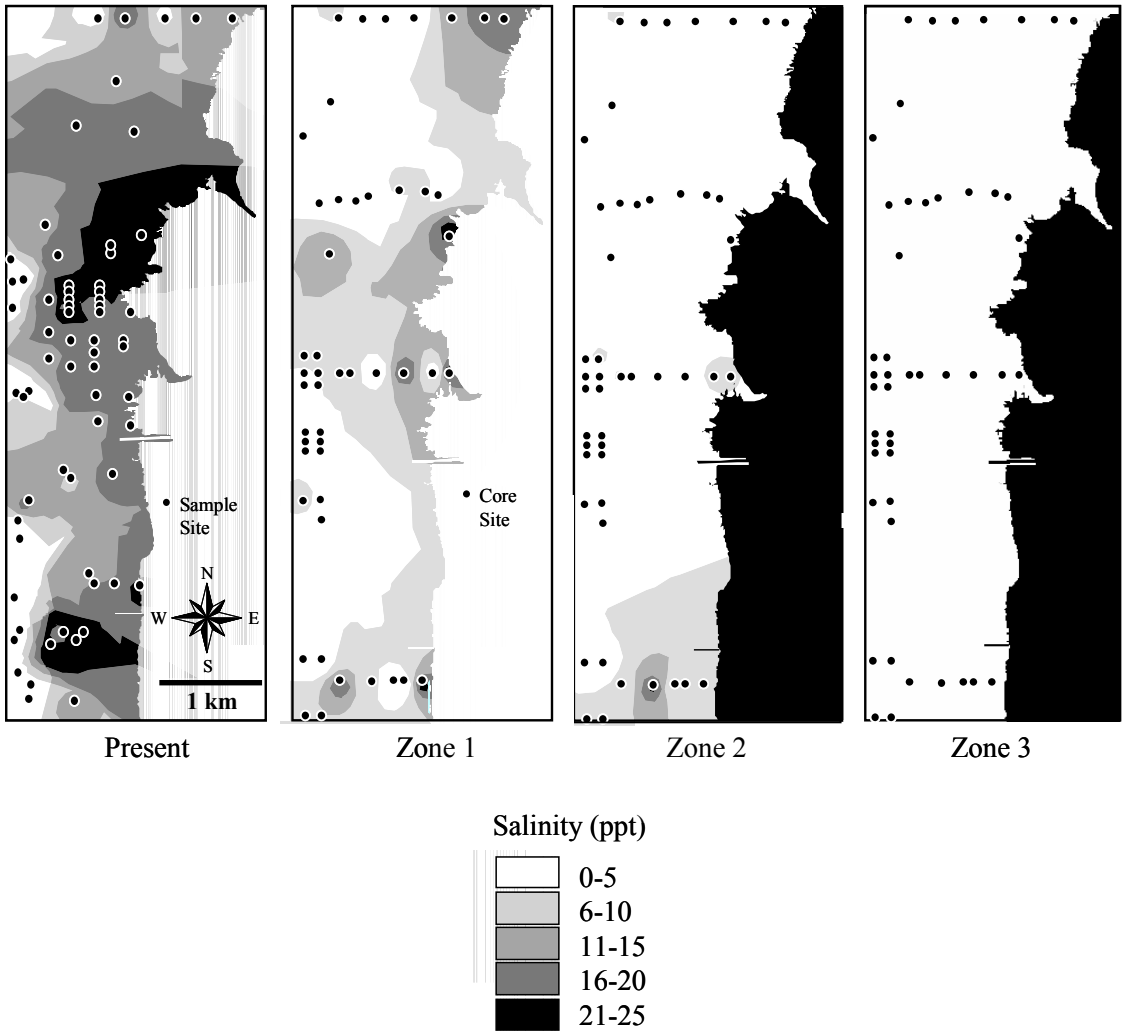
Sample Site
Core Site
N
W
E
S
1 km
Present
Zone 1
Zone 2
Zone 3
Salinity (ppt)
0-5
6-10
11-15
16-20
21-25

Figure 9

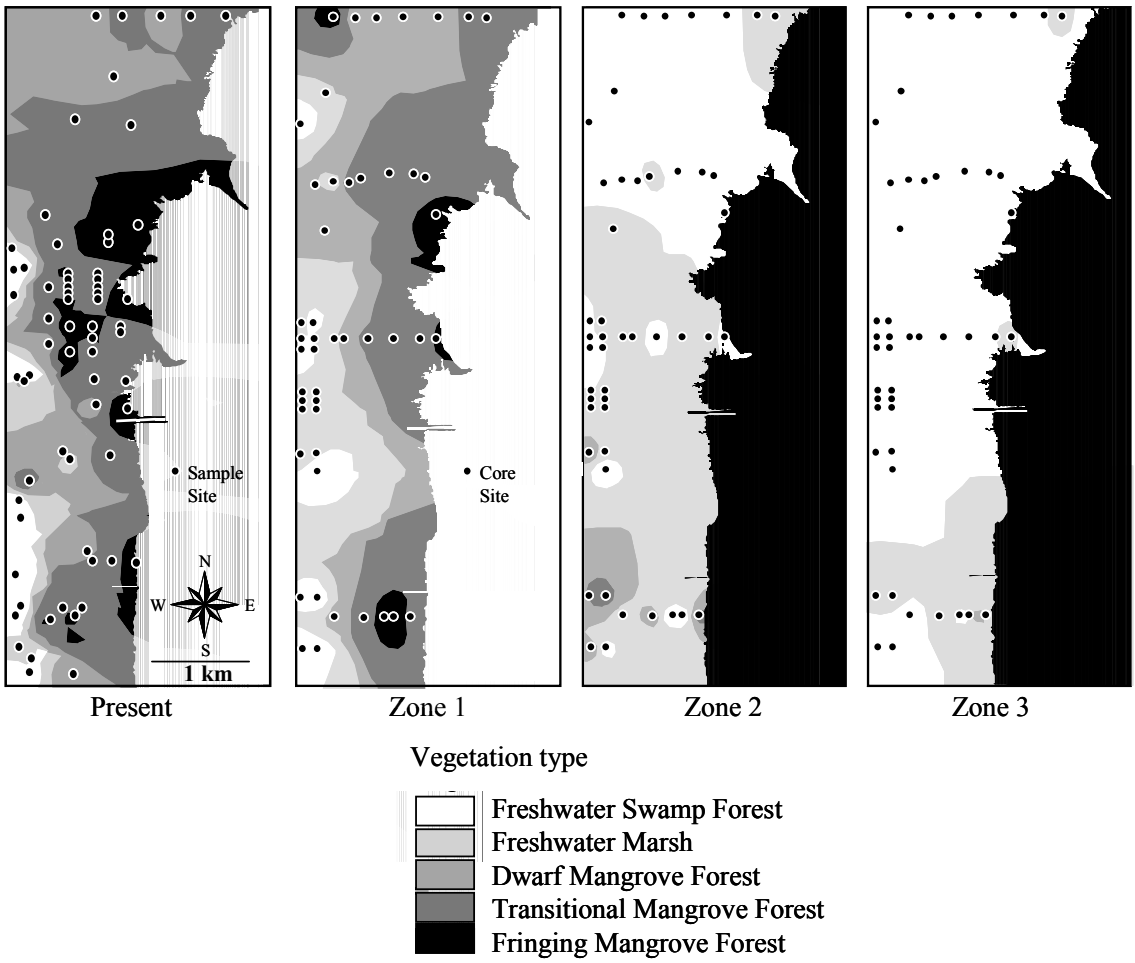
Sample Site
Core Site
N
W
E
S
1 km
Present
Zone 1
Zone 2
Zone 3
Vegetation type
Freshwater Swamp Forest
Freshwater Marsh
Dwarf Mangrove Forest
Transitional Mangrove Forest
Fringing Mangrove Forest

Figure 10

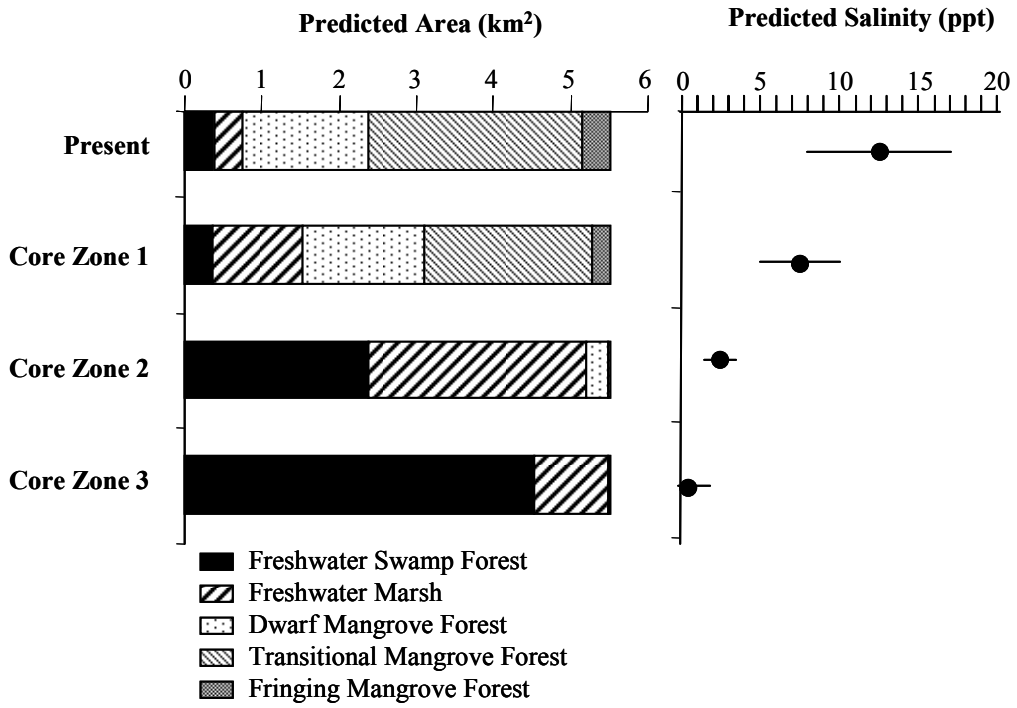
Predicted Area (km²)
Predicted Salinity (ppt)
0
1
2
3
4
5
6
0
5
10
15
20
Present
Core Zone 1
Core Zone 2
Core Zone 3
Freshwater Swamp Forest
Freshwater Marsh
Dwarf Mangrove Forest
Transitional Mangrove Forest
Fringing Mangrove Forest